第 9 1 卷　第 1 2 期
2017年12月　2854～2866

地　质　学　报　ACTA GEOLOGICA SINICA

Vol. 91 No. 12 2017
Dec. 2854～2866

黑龙江五大连池火山口湖沉积物有机残体粒度记录的早全新世千百年尺度夏季风降水演化

刘孝艳[1)]，詹涛[2)]，刘恋[3)]，周鑫[1)]，乔彦松[4)]，涂路遥[1)]，马永法[2)]，姜侠[5)]，张俊[2)]，娄本军[2)]

1）中国科学技术大学地球和空间科学学院，合肥，230026；
2）黑龙江省第二水文地质工程地质勘察院，哈尔滨，150030；
3）中国地质科学院，北京，100037；4）中国地质科学院地质力学研究所，北京，100081；
5）黑龙江省地质矿产局，哈尔滨，150036

内容提要：目前已在我国大量地质记录中发现全新世早期的千百年尺度气候事件，但较高纬度地区相应的记录仍较少。因此，有必要在我国较高纬度地区进行千百年尺度气候事件的重建。本文对五大连池火山口湖沉积物进行研究，以精确的^{14}C年代框架为基础，对沉积物(未去除有机残体)粒度数据进行粒级－标准偏差分析，提取了＞83 μm 敏感粒级，发现该粒级主要成分为有机残体，其粒度和含量可作为夏季风降水代用指标，进而利用该组分重建了我国东北地区早全新世夏季风降水演化历史。结果表明，我国东北地区早全新世季风降水频繁波动，存在～8.6 ka，9.2 ka，10.2 ka 和 11.6 ka 四次千百年尺度显著弱夏季风事件。在年代误差范围内，四次弱夏季风事件与我国季风区其他气候记录、北大西洋冰筏沉积及太阳活动记录在时间上均有较好的一致性，指示早全新世千百年尺度干旱事件在我国季风区普遍存在，且与北大西洋浮冰事件及太阳活动密切相关。但五大连池火山口湖有机残体粒度记录的四次千百年尺度弱夏季风事件持续时间明显短于其他气候记录中的相应事件，初步推测为北大西洋浮冰事件通过影响热带季风进而影响较高纬度地区，季风信号从低纬传输至高纬变弱，致使事件持续时间明显缩短。

关键词：早全新世；火山口湖；敏感粒级；弱夏季风事件；中国东北地区

研究过去气候变化规律和机制对于预测未来气候变化趋势及探索人地关系具有至关重要的作用(Hou Guangliang et al., 2011)。早期研究(Jouzel et al., 1987; Dansgaard et al., 1993)认为，新仙女木事件结束(～11500 a BP)后为平稳回暖的早全新世阶段。然而，自 Bond et al. (1997)发现北大西洋冷事件后，全球范围内陆续问世的大量古气候指标证实，全新世早期存在多个千百年尺度的气候事件(Wang Ninglian et al., 2002; Mayewski et al., 2004; Rasmussen et al., 2007; Wang Shaowu et al., 2013)，其气候不稳定性引起了国内外的广泛关注。

目前，国内对于早全新世千百年尺度气候变化的研究集中于夏季风演化方面，研究材料包括石笋、湖泊沉积物和泥炭等。湖南莲花洞(Zhang Huiling et al., 2013; Zhang Huasheng et al., 2016)、贵州董歌洞(Dykoski et al., 2005)、竹蹓坪洞(Huang Wei et al., 2016)及豫西老母洞(Zhang Yinhuan et al., 2015)等的高分辨率石笋 $\delta^{18}O$ 记录中均识别出早全新世存在多次千百年尺度弱夏季风事件，其中 8.2 ka BP 和 9.2 ka BP 的弱夏季风事件在我国季风区普遍存在。此外，中国西北季风边缘区民勤盆地湖泊沉积(Chen Fahu et al., 2001)记录中也发现早全新世夏季风波动具有明显的 800 年周期。青海湖沉积物记录(Liu Xingxing et al., 2016)中也识别出了早全新世的 4 次弱夏季风事件，且和北大西洋冷事件及太阳活动有很好的对应关系。我国东北哈尼泥炭纤维素 $\delta^{13}C$ 记录(Hong Yetang et al.,

注：本文为国土资源部公益性科研专项(201311137)，国家重点基础研究发展规划项目(973 项目)(批准号：2010CB428902)，国家自然科学基金项目(批准号：41301040、41672159、41102223，41306198)，黑龙江省青年科学基金项目(批准号：QC2013C039)和中国地质科学院基本科研业务费项目(批准号：ywf201609)共同资助的成果。
收稿日期：2016-10-28；改回日期：2017-01-18；责任编辑：黄敏。
作者简介：刘孝艳，女，1993 年生。硕士研究生，环境科学专业。Email：ylian@mail.ustc.edu.cn。通讯作者：周鑫，男，副教授。Email：xinzhou@ustc.edu.cn。

2005)也揭示了一系列千年尺度季风突变事件,且与北大西洋冷事件相对应。虽然上述研究确认了我国全新世早期千百年尺度弱夏季风事件的存在,但仍存在一定不足。首先,在时间跨度上,相关序列大多覆盖整个全新世,缺乏对早全新世突变事件的精确探讨(Zhang Huasheng et al., 2016);其次,在空间分布上,早全新世较高纬度季风区记录相对较少,且分辨率低,限制了高低纬之间的深入对比研究(Cai Binggui et al., 2008);第三,常用于研究全新世早期千百年尺度夏季风事件的石笋氧同位素指示意义尚不明确,石笋氧同位素究竟指示东亚季风(Liu Zhengyu et al., 2014)还是印度季风(Liu Jianbao et al., 2015),降雨量还是降雨来源,目前仍存在不同观点(Tan Ming, 2014);此外,早全新世千百年尺度弱夏季风事件的成因机制仍有待进一步研究。因此,要深入探讨早全新世夏季风演化的时空规律及驱动机制,还需在不同地区获取理想的研究材料并寻找对沉积环境敏感的气候指标。

湖泊沉积物是古气候研究的重要地质档案(Duan Yi et al., 2016; Li Suping et al., 2016; Liu Siwen et al., 2016),其中火山口湖沉积物因具有湖盆封闭、汇水区域小以及不受河流输入干扰等独特的优势而被广泛应用于古气候重建(Liu Qiang et al., 2010; Gui Zhifan et al., 2011; Liu Jiali et al., 2015)。粒度是古气候研究中重要的物理指标,常用于指示沉积环境变化(Li Jiacai et al., 2015),进而用于重建古环境演化(Li Huayong et al., 2014; Tu Luyao et al., 2015; Zheng Wenxin et al., 2015; Liu Zhirong et al., 2016; Tu Luyao et al., 2016)。

我国东北大部分地区属于典型季风区,是重要的商品粮食基地,区域气候变化与人类生产生活密切相关(Shen Baizhu et al., 2011),因此对该区域季风事件的研究具有显著的科学和现实意义。本文拟通过对该区域五大连池火山口湖沉积物粒度数据进行分析,重建早全新世夏季风演化,并与其他气候记录进行对比,进而探讨可能的驱动机制。

1　材料与方法

1.1　地质背景与样品采集

南格拉球山(126.00°E, 48.74°N)位于我国东北黑龙江省五大连池风景区内,是一座相对地面高度约 150 m 的火山,海拔 596.9 m。五大连池天池是南格拉球山山顶的一个封闭湖泊,直径约 500 m。由于 20 世纪 70 年代山顶被炸开放水,目前湖泊出现显著的沼泽化,其中生长了大量的水生植物。该地区目前为典型的寒温带季风区,其气候受大兴安岭寒温带湿润气候和松嫩平原温带半湿润、半干旱气候的综合影响,冬季严寒漫长,夏季凉爽短促。年均气温 0～0.5℃,年均降水量约为 470 mm,多集中在 6～8 月。五大连池天池位于东亚季风区,对气候变化较为敏感,且受人为因素干扰较小,是研究早全新世东亚季风演变历史的理想地点。

沉积柱 TC1 于 2011 年 11 月使用重力钻获得,钻孔位置如图 1 所示。沉积柱长 197 cm,按 0.5 cm 间隔分样。岩心岩性组成大致可分为两段:0～125 cm 为灰黄色黏土,含较多有机质残体,其中 16～18 cm 处存在一层黑色火山灰;125～197 cm 为黑色黏土,同样含有大量有机质残体,但残体均较为细小。

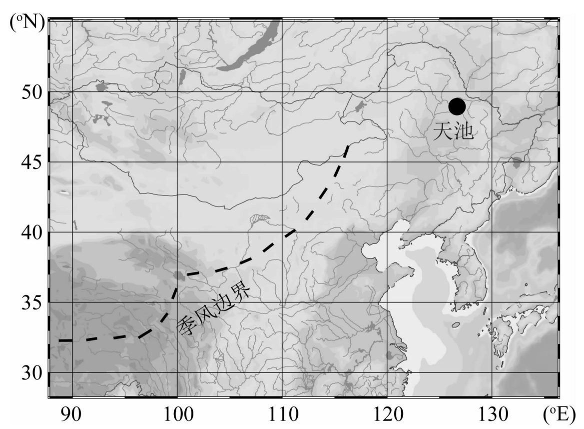

图 1　黑龙江五大连池火山口湖位置图

Fig. 1　Location of Wudalianchi Crater Lake in Heilongjiang Province

1.2　分析方法

选取 TC1 沉积柱中不同深度的 16 个样品进行 AMS ^{14}C 测年,定年材料包括全岩有机碳、植物叶片等残体和种子(Zhou Xin et al., 2016),分别在美国佐治亚大学及加拿大渥太华大学进行(表 1)。测年结果使用 IntCal13 (Reimer et al., 2013)进行校正。

粒度分析在中国科学技术大学极地环境研究室完成,所用仪器为 LS13320 型激光粒度仪,测量范围为 2～2000 μm,粒级分辨率为 0.01Φ,重复测试的相对误差<2%。具体操作如下:取适量沉积物样品加少量 30% H_2O_2,摇匀并用电热板加热至 150℃以除去部分易氧化有机质,保留有机残体的主要部分,然后加入 10 mL 10%的 HCl 除去碳酸盐,静置 48 小时,再加入 10 mL 10%的六偏磷酸钠(分

散剂)，超声 10 分钟使样品颗粒充分分散后上机测试。

表 1 黑龙江五大连池火山口湖 TC1 沉积物 AMS ^{14}C 定年结果
Table 1 Radiocarbon dates of Core TC1 from Wudalianchi Crater Lake in Heilongjiang Province

实验室编号	定年材料	深度(cm)	校正年龄(cal a BP)	误差
10110	全岩有机碳	16	210	90
13190	种子	24.5	690	20
13194	种子	29	1470	50
10111	全岩有机碳	41.5	2830	40
UOC-1162	叶片	52	4017	123
13191	植物残体	65	4740	70
13192	植物残体	83	6360	40
UOC-1163	叶片	90.5	6976	180
10112	全岩有机碳	101	7290	30
10114	全岩有机碳	120	7990	30
10113	全岩有机碳	147	9070	40
10115	全岩有机碳	161	9850	80
13194	种子	177	10240	20
13195	种子	184	13120	70
10116	全岩有机碳	197	13730	50
13196	植物残体	197	12690	30

注：实验室编号为 UOC 的样品在加拿大渥太华大学测试；其它样品在佐治亚大学测试。

采用粒级－标准偏差变化曲线法对沉积物粒度进行多组分分离，提取对环境变化敏感的粒度组分。粒度－标准偏差曲线法能够依据不同样品每一粒级对应的粒度含量的标准偏差变化来获取粒度敏感组分(Chen Qiao et al.，2013)。某一粒级所对应的标准偏差值越大，说明该粒级对应的粒度含量差异较大，对沉积环境变化越敏感；反之，标准偏差值越小，说明该粒级对环境变化越不敏感(He Jishan et al.，2015)。这一方法目前已被广泛用于古环境重建(Xiao Shangbin et al.，2005；Xiang Rong et al.，2006；Zhou Xin et al.，2014；Tu Luyao et al.，2016)。

2 分析结果

2.1 年代学框架

校正后的深度－年代曲线如图 2 所示。采用线性内插法建立起五大连池天池沉积物年代学标尺，钻孔底部年龄为 13991 a BP。不同深度范围沉积速率存在一定差异：0～16 cm，16～83 cm，83～177 cm，177～184 cm 以及 184 cm 至最底部沉积速率分别为 0.076 cm・a^{-1}、0.011 cm・a^{-1}、0.024 cm・a^{-1}、0.002 cm・a^{-1}和 0.021 cm・a^{-1}。沉积柱 197 cm 深度处植物残体测得的年代较全岩有机碳测得年代显著偏轻，可能由于钻取岩心时钻头部位带入上部残体所致。此外，16～18 cm 处火山灰年代和^{14}C 年代较为吻合(Zhou Xin et al.，2016)，且 12000 a BP 以来的植物残体年代与全岩年代均无倒置现象(表 1)，表明沉积物年代基本不受碳库效应影响。

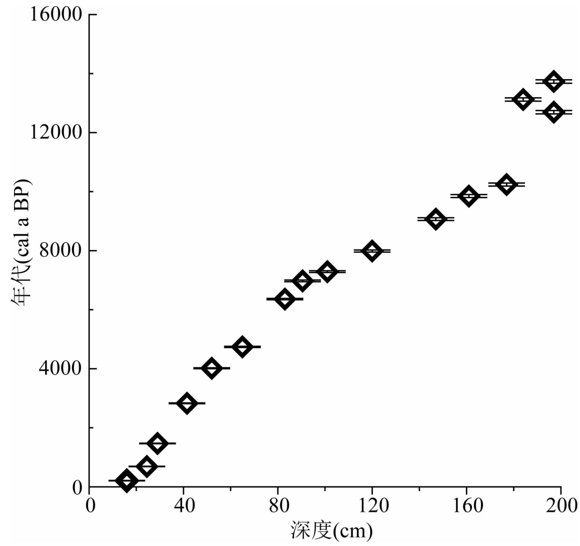

图 2 黑龙江五大连池火山口湖沉积物 TC1 沉积柱深度－年代分布
Fig. 2 Depth-age distribution of Core TC1 from Wudalianchi Crater Lake in Heilongjiang Province

2.2 粒度分布及粒级－标准偏差变化曲线

沉积物粒度频率分布曲线能够直观、清晰地反映粒度组分信息及分布(Xue Jibin et al.，2008；Tu Luyao et al.，2015；Peng Shuzhen et al.，2016)特征等。由图 3 可见，TC1 孔下部沉积物样品粒度频率分布曲线均呈多峰分布，且粒度分布区间相似，表明沉积环境类似。

同一沉积环境下的沉积物粒度组成受到搬运过程中物源和动力条件等因素的影响(Yang Zuosheng et al.，2007)。在复杂沉积条件下运用沉积物粒度数据解释古环境变化(Xiang Rong et al.，2006；Huang Jie et al.，2011；Li Chaozhu et al.，2015)时，相对于沉积物全岩粒度而言，敏感粒级组分因具有更明确的环境指示意义而被广泛应用。使用粒级－标准偏差曲线法对 TC1 孔沉积物粒度数据进行分析，得到了不同粒度组分的标准偏差随粒级的变化。TC1 孔粒级－标准偏差曲线呈现典型的多峰分布(图 3，表 2)，说明沉积环境可能受多种因素控制。图中四个标准偏差峰值分别出现在粒径为 0.2 μm、9.8 μm、33.0 μm 和 339.9 μm 处，所对

应的粒度组分范围分别为<0.7 μm (组分 1)、0～23 μm (组分 2)、23～83 μm (组分 3)和>83 μm (组分 4)。由粒度频率分布曲线可知,组分 1 含量较低,因此在本研究中不予考虑。

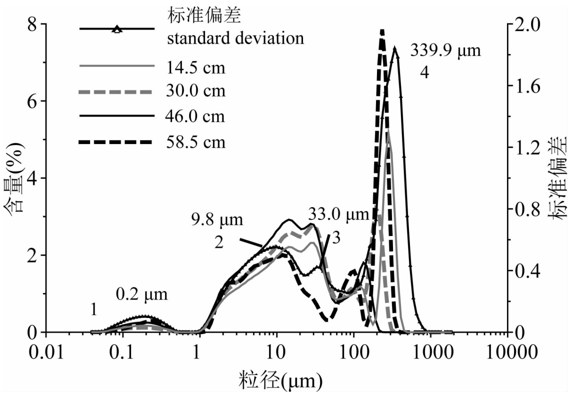

图 3　黑龙江五大连池火山口湖沉积物 TC1 孔不同深度沉积物粒度频率分布曲线及标准偏差变化

Fig. 3　Grain-size frequency and standard deviation in sediments of Core TC1 from Wudalianchi Crater Lake in Heilongjiang Province

图中 4 条不同线型曲线为不同深度沉积物粒度频率分布曲线;三角点黑色曲线为标准偏差变化曲线,数字 1～4 代表 4 个粒度组分

Four different lines show frequency distribution of sediments at different depths, and the black line with triangle dots shows grain size versus standard deviation curve. The numbers 1, 2, 3 and 4 are four components indicated by the grain size versus standard deviation curve

3　讨论

3.1　敏感粒级的指示意义

敏感粒级组分的主要来源是确定其气候指示意义的关键。TC1 孔含有机残体与不含有机残体的典型沉积物样品粒度频率分布曲线(图 4,表 3)对比结果表明,未去除有机残体的沉积物粒度频率分布曲线中组分 4 (>83 μm 组分)含量较高,而去除有机残体后的沉积物粒度频率分布曲线中基本不含该组分,因此敏感粒级组分 4 主要成分为有机残体。

组分 4 中值粒径与烧失量在岩心剖面上的变化趋势显著一致(图 5),说明两者具有类似的气候指示意义;但敏感粒级组分中值粒径的变化幅度较大,具有明显的千百年尺度变化特征,表明该指标对沉积环境变化更为敏感。已有研究(Zhou Xin et al., 2016)表明,天池沉积物 550 ℃烧失量和树木孢粉含量变化趋势一致,两者均指示季风降水变化。因此,敏感粒级组分 4 也应指示了季风降水的变化。首先,夏季风增强时,降雨增多,气候暖湿,初级生产力提高,使得更多有机质进入湖泊;再者,降水增多时,

表 2　黑龙江五大连池火山口湖 TC1 沉积柱不同深度沉积物粒度含量及标准偏差分析结果

Table 2　Grain size contents at different depths and standard deviation in sediment of Core TC1 from Wudalianchi Crater Lake in Heilongjiang Province

粒级 (μm)	标准偏差	含量(%)			
		14.5 cm	30 cm	46 cm	58.5 cm
0.0400	0.0013	0.0023	0.0016	0.0035	0.0009
0.0439	0.0017	0.0030	0.0021	0.0045	0.0013
0.0482	0.0027	0.0047	0.0032	0.0071	0.0023
0.0529	0.0052	0.0093	0.0064	0.0142	0.0046
0.0581	0.0110	0.0196	0.0134	0.0297	0.0095
0.0638	0.0207	0.0364	0.0250	0.0551	0.0176
0.0700	0.0320	0.0554	0.0382	0.0834	0.0284
0.0768	0.0422	0.0725	0.0502	0.1089	0.0410
0.0844	0.0515	0.0882	0.0610	0.1322	0.0554
0.0926	0.0610	0.1042	0.0720	0.1560	0.0728
0.1017	0.0702	0.1196	0.0826	0.1790	0.0932
0.1116	0.0783	0.1330	0.0917	0.1988	0.1152
0.1225	0.0851	0.1445	0.0995	0.2158	0.1377
0.1345	0.0910	0.1540	0.1060	0.2300	0.1616
0.1476	0.0956	0.1613	0.1108	0.2408	0.1878
0.1621	0.0988	0.1662	0.1139	0.2481	0.2146
0.1779	0.1008	0.1691	0.1156	0.2522	0.2400
0.1953	0.1013	0.1695	0.1157	0.2528	0.2627
0.2144	0.0998	0.1664	0.1133	0.2483	0.2816
0.2354	0.0959	0.1591	0.1081	0.2377	0.2934
0.2584	0.0896	0.1486	0.1007	0.2217	0.2926
0.2836	0.0811	0.1345	0.0912	0.2010	0.2763
0.3113	0.0705	0.1173	0.0795	0.1755	0.2468
0.3418	0.0582	0.0964	0.0656	0.1451	0.2085
0.3752	0.0455	0.0764	0.0519	0.1145	0.1565
0.4119	0.0322	0.0554	0.0383	0.0837	0.0906
0.4521	0.0185	0.0327	0.0231	0.0499	0.0340
0.4963	0.0074	0.0126	0.0094	0.0203	0.0062
0.5449	0.0015	0.0024	0.0019	0.0041	0.0004
0.5981	0.0001	0.0002	0.0001	0.0003	0
0.6566	0	0	0	0	0
0.7208	0	0	0	0	0
0.7913	0	0	0	0	0
0.8686	0.0004	0.0007	0.0007	0.0006	0
0.9536	0.0039	0.0095	0.0095	0.0094	0
1.0468	0.0188	0.0508	0.0516	0.0539	0.0006
1.1491	0.0447	0.1348	0.1399	0.1551	0.0115
1.2615	0.0761	0.2537	0.2683	0.3088	0.0735
1.3848	0.1030	0.3768	0.4046	0.4788	0.2374
1.5202	0.1358	0.5075	0.5520	0.6607	0.4918
1.6688	0.1733	0.6334	0.6963	0.8376	0.7630
1.8319	0.2136	0.7537	0.8372	1.0091	0.9922
2.0110	0.2514	0.8543	0.9592	1.1558	1.1480
2.2076	0.2858	0.9384	1.0635	1.2804	1.2441
2.4234	0.3161	1.0046	1.1475	1.3774	1.2798
2.6603	0.3417	1.0582	1.2133	1.4519	1.2889
2.9204	0.3675	1.1131	1.2787	1.5248	1.2855
3.2059	0.3903	1.1617	1.3339	1.5882	1.3022
3.5193	0.4158	1.2258	1.4059	1.6725	1.3664

续表 2

粒级 (μm)	标准偏差	含量(%)			
		14.5 cm	30 cm	46 cm	58.5 cm
3.8634	0.4363	1.2782	1.4637	1.7413	1.4538
4.2411	0.4585	1.3480	1.5398	1.8318	1.5694
4.6557	0.4747	1.3972	1.5932	1.8946	1.6426
5.1109	0.4922	1.4608	1.6625	1.9767	1.7121
5.6105	0.5052	1.5084	1.7171	2.0400	1.7378
6.1590	0.5178	1.5698	1.7880	2.1220	1.7802
6.7611	0.5284	1.6305	1.8604	2.2037	1.8109
7.4221	0.5371	1.6945	1.9366	2.2892	1.8394
8.1477	0.5467	1.7769	2.0340	2.3981	1.8767
8.9443	0.5499	1.8475	2.1197	2.4901	1.8912
9.8187	0.5535	1.9477	2.2386	2.6174	1.9435
10.7786	0.5469	2.0198	2.3270	2.7039	1.9642
11.8323	0.5417	2.1158	2.4419	2.8174	2.0035
12.9891	0.5281	2.1718	2.5133	2.8781	1.9814
14.2589	0.5120	2.2120	2.5717	2.9203	1.9023
15.6529	0.4867	2.2018	2.5755	2.8986	1.7527
17.1832	0.4526	2.1523	2.5357	2.8213	1.5403
18.8630	0.4162	2.1082	2.4943	2.7399	1.3379
20.7071	0.3825	2.0872	2.4697	2.6719	1.1588
22.7315	0.3685	2.1423	2.5252	2.6900	1.0476
24.9538	0.3711	2.2283	2.6177	2.7456	0.9764
27.3934	0.3879	2.3153	2.7261	2.8122	0.9196
30.0714	0.4066	2.3180	2.7581	2.7895	0.8374
33.0113	0.4220	2.2000	2.6703	2.6268	0.7087
36.2385	0.4196	1.9566	2.4382	2.3081	0.5495
39.7813	0.3942	1.6368	2.0910	1.8813	0.4029
43.6704	0.3556	1.3191	1.6951	1.4443	0.3177
47.9397	0.3199	1.0655	1.3207	1.0847	0.3166
52.6264	0.2938	0.9125	1.0326	0.8597	0.4090
57.7713	0.2761	0.8506	0.8557	0.7636	0.5852
63.4192	0.2681	0.8537	0.7929	0.7647	0.8095
69.6192	0.2653	0.8836	0.8254	0.8131	1.0347
76.4253	0.2597	0.9109	0.9271	0.8639	1.2353
83.8969	0.2538	0.9310	1.0486	0.9117	1.4033
92.0988	0.2618	0.9607	1.1217	0.9858	1.5448
101.1030	0.2847	1.0247	1.0818	1.1337	1.5823
110.9870	0.3004	1.1245	0.9252	1.3733	1.3885
121.8370	0.3093	1.1862	0.7884	1.6416	0.8762
133.7480	0.3670	1.0964	0.8108	1.8060	0.3456
146.8240	0.4723	0.7676	1.1421	1.7189	0.1757
161.1770	0.5564	0.3657	1.8147	1.3387	0.4276
176.9350	0.5810	0.2015	2.6453	0.7653	1.7601
194.2320	0.7292	0.3446	3.1937	0.2860	4.3140
213.2210	1.0817	1.1774	3.0902	0.0526	6.8996
234.0660	1.3914	2.7733	2.3136	0.0037	7.8556
256.9480	1.5585	4.4656	1.2310	0	6.8829
282.0680	1.6400	5.1589	0.4094	0	4.3112
309.6440	1.7539	4.6345	0.0672	0	1.7806
339.9160	1.8405	3.1056	0.0037	0	0.3560
373.1470	1.7836	1.4382	0	0	0.0293
409.6260	1.5274	0.3806	0	0	0
449.6720	1.1395	0.0484	0	0	0
493.6330	0.7542	0.0012	0	0	0
541.8920	0.4321	0	0	0	0

续表 2

粒级 (μm)	标准偏差	含量(%)			
		14.5 cm	30 cm	46 cm	58.5 cm
594.8690	0.2209	0	0	0	0
653.0250	0.1168	0	0	0	0
716.8660	0.0663	0	0	0	0
786.9490	0.0306	0	0	0	0
863.8830	0.0094	0	0	0	0
948.3380	0.0016	0	0	0	0
1041.0500	0.0001	0	0	0	0
1142.8300	0	0	0	0	0
1254.5500	0	0	0	0	0
1377.2000	0	0	0	0	0
1511.8400	0	0	0	0	0
1659.6400	0	0	0	0	0
1821.8900	0	0	0	0	0

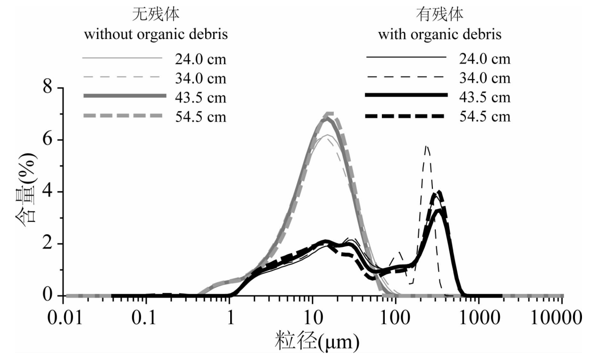

图 4 黑龙江五大连池火山口湖 TC1 沉积柱不同深度有无有机残体的沉积物样品粒度频率分布曲线

Fig. 4 Distribution of grain-size frequency of sediment samples with and without organic debris at different depths in Core TC1 from Wudalianchi Crater Lake in Heilongjiang Province

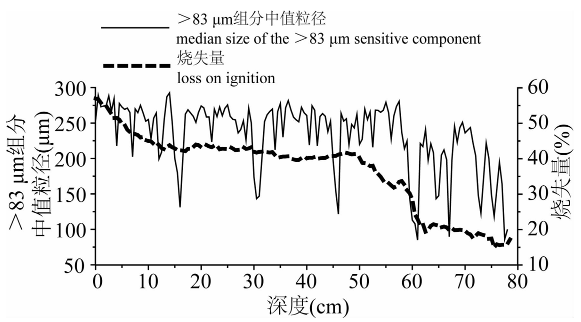

图 5 黑龙江五大连池火山口湖 TC1 孔敏感粒级组分中值粒径与 550 ℃烧失量(Zhou Xin et al., 2016)的对比

Fig. 5 Comparison between median size of the sensitive component and LOI 550℃ (Zhou Xin et al., 2016) in Core TC1 from Wudalianchi Crater Lake in Heilongjiang Province

湖水深度增加,还原环境更利于有机残体的保存,因此有机残体含量多且粒径大,这也与前人(Blackford et al., 1995; Borgmark et al., 2005; Ma Chunmei et al., 2009)所用的腐殖化度指标较

表 3　黑龙江五大连池火山口湖 TC1 沉积柱不同深度有无有机残体的沉积物样品粒度含量

Table 3　Grain size content at different depths in sediments with and without organic debris of Core TC1 from Wudalianchi Crater Lake in Heilongjiang Province

粒级 2	含量(%)				粒级 1	含量(%)			
	24 cm	34 cm	43.5 cm	54.5 cm		24 cm	34 cm	43.5 cm	54.5 cm
0.0115	0	0	0	0	0.0400	0	0.0010	0	0
0.0132	0	0	0	0	0.0439	0	0.0014	0	0
0.0151	0	0	0	0	0.0482	0	0.0023	0	0
0.0174	0	0	0	0	0.0529	0	0.0045	0	0
0.0200	0	0	0	0	0.0581	0	0.0094	0	0
0.0229	0	0	0	0	0.0638	0	0.0175	0	0
0.0263	0	0	0	0	0.0700	0	0.0269	0	0
0.0302	0	0	0	0	0.0768	0	0.0358	0	0
0.0347	0	0	0	0	0.0844	0	0.0439	0	0
0.0398	0	0	0	0	0.0926	0	0.0525	0	0
0.0457	0	0	0	0	0.1017	0	0.0610	0	0
0.0525	0	0	0	0	0.1116	0	0.0682	0	0
0.0603	0	0	0	0	0.1225	0	0.0744	0	0
0.0692	0	0	0	0	0.1345	0	0.0802	0	0
0.0794	0	0	0	0	0.1476	0	0.0854	0	0
0.0912	0	0	0	0	0.1621	0	0.0892	0	0
0.1047	0	0	0	0	0.1779	0	0.0913	0	0
0.1202	0	0	0	0	0.1953	0	0.0919	0	0
0.1380	0	0	0	0	0.2144	0	0.0909	0	0
0.1585	0	0	0	0	0.2354	0	0.0874	0	0
0.1820	0	0	0	0	0.2584	0	0.0802	0	0
0.2089	0	0	0	0	0.2836	0	0.0698	0	0
0.2399	0	0	0	0	0.3113	0	0.0586	0	0
0.2754	0	0	0	0	0.3418	0	0.0463	0	0
0.3162	0	0	0	0	0.3752	0	0.0296	0	0
0.3631	0	0	0	0	0.4119	0	0.0130	0	0
0.4169	0	0	0	0	0.4521	0	0.0027	0	0
0.4786	0.1267	0.1451	0.1158	0.1346	0.4963	0	0.0002	0	0
0.5495	0.2470	0.2741	0.2302	0.2564	0.5449	0	0	0	0
0.6310	0.3718	0.4013	0.3481	0.3758	0.5981	0	0	0	0
0.7244	0.4581	0.4870	0.4281	0.4514	0.6566	0	0	0	0
0.8318	0.5256	0.5557	0.4892	0.5052	0.7208	0	0	0	0
0.9550	0.5694	0.6026	0.5277	0.5338	0.7913	0	0	0	0
1.0965	0.6059	0.6440	0.5598	0.5543	0.8686	0.0001	0	0.0002	0
1.2589	0.6489	0.6926	0.5996	0.5812	0.9536	0.0031	0	0.0046	0.0010
1.4454	0.7152	0.7645	0.6636	0.6310	1.0468	0.0214	0.0012	0.0292	0.0130
1.6596	0.8149	0.8690	0.7618	0.7133	1.1491	0.0745	0.0157	0.0939	0.0680
1.9055	0.9534	1.0110	0.8988	0.8316	1.2615	0.1661	0.0836	0.1992	0.1792
2.1878	1.1276	1.1881	1.0707	0.9814	1.3848	0.2781	0.2224	0.3225	0.3304
2.5119	1.3361	1.4012	1.2754	1.1600	1.5202	0.3968	0.4100	0.4532	0.4858
2.8840	1.5811	1.6555	1.5155	1.3698	1.6688	0.5104	0.5872	0.5795	0.6349
3.3113	1.8687	1.9599	1.7986	1.6191	1.8319	0.6189	0.7407	0.7010	0.7760
3.8019	2.2066	2.3239	2.1366	1.9202	2.0110	0.7098	0.8530	0.8036	0.8945
4.3652	2.5969	2.7487	2.5370	2.2832	2.2076	0.7869	0.9332	0.8911	0.9961
5.0119	3.0433	3.2351	3.0106	2.7219	2.4234	0.8440	0.9779	0.9575	1.0718
5.7544	3.5317	3.7626	3.5491	3.2336	2.6603	0.8864	1.0007	1.0084	1.1288
6.6069	4.0545	4.3159	4.1497	3.8222	2.9204	0.9263	1.0120	1.0573	1.1812
7.5858	4.5776	4.8506	4.7756	4.4588	3.2059	0.9617	1.0278	1.1009	1.2307
8.7096	5.0837	5.3396	5.4043	5.1281	3.5193	1.0114	1.0718	1.1600	1.2982
10.0000	5.5264	5.7302	5.9714	5.7690	3.8634	1.0519	1.1206	1.2087	1.3559
11.4815	5.8844	5.9969	6.4381	6.3445	4.2411	1.1066	1.1895	1.2734	1.4274

续表 3

粒级 2	含量(%)				粒级 1	含量(%)			
	24 cm	34 cm	43.5 cm	54.5 cm		24 cm	34 cm	43.5 cm	54.5 cm
13.1826	6.1153	6.1051	6.7352	6.7754	4.6557	1.1421	1.2273	1.3172	1.4732
15.1356	6.2012	6.0457	6.8256	7.0146	5.1109	1.1905	1.2735	1.3752	1.5307
17.3780	6.1243	5.8241	6.6792	7.0094	5.6105	1.2260	1.2974	1.4189	1.5694
19.9526	5.8804	5.4554	6.2916	6.7371	6.1590	1.2763	1.3460	1.4777	1.6207
22.9087	5.4841	4.9783	5.6968	6.2109	6.7611	1.3273	1.3949	1.5366	1.6672
26.3027	4.9506	4.4223	4.9369	5.4626	7.4221	1.3829	1.4503	1.5994	1.7138
30.1995	4.3185	3.8308	4.0898	4.5696	8.1477	1.4561	1.5262	1.6799	1.7743
34.6737	3.6199	3.2287	3.2194	3.6048	8.9443	1.5220	1.5979	1.7496	1.8201
39.8107	2.9028	2.6442	2.3985	2.6653	9.8187	1.6179	1.7216	1.8482	1.8926
45.7088	2.2078	2.0928	1.6755	1.8136	10.7786	1.6938	1.8319	1.9205	1.9355
52.4807	1.5763	1.5889	1.0833	1.1124	11.8323	1.7937	1.9723	2.0141	1.9966
60.2560	1.0424	1.1459	0.6342	0.6214	12.9891	1.8584	2.0527	2.0660	2.0130
69.1831	0.6217	0.7729	0.3303	0.0225	14.2589	1.9078	2.0813	2.0985	2.0038
79.4328	0.3341	0.4787	0.1253	0	15.6529	1.9126	2.0365	2.0810	1.9411
91.2011	0.1328	0.2711	0.0232	0	17.1832	1.8875	1.9500	2.0252	1.8334
104.7129	0.0319	0.1228	0	0	18.8630	1.8729	1.8981	1.9723	1.7274
120.2264	0	0.0371	0	0	20.7071	1.8836	1.9041	1.9319	1.6333
138.0384	0	0	0	0	22.7315	1.9598	2.0074	1.9476	1.5986
158.4893	0	0	0	0	24.9538	2.0555	2.1429	1.9762	1.5882
181.9701	0	0	0	0	27.3934	2.1428	2.2582	1.9982	1.5844
208.9296	0	0	0	0	30.0714	2.1508	2.2720	1.9525	1.5331
239.8833	0	0	0	0	33.0113	2.0622	2.1723	1.8240	1.4124
275.4229	0	0	0	0	36.2385	1.8842	1.9842	1.6215	1.2275
316.2278	0	0	0	0	39.7813	1.6635	1.7682	1.3880	1.0149
363.0781	0	0	0	0	43.6704	1.4539	1.5727	1.1782	0.8284
416.8694	0	0	0	0	47.9397	1.2877	1.4152	1.0267	0.7057
478.6301	0	0	0	0	52.6264	1.1787	1.2915	0.9482	0.6626
549.5409	0	0	0	0	57.7713	1.1112	1.1804	0.9282	0.6875
630.9573	0	0	0	0	63.4192	1.0687	1.0845	0.9452	0.7565
724.4360	0	0	0	0	69.6192	1.0364	1.0229	0.9756	0.8358
831.7638	0	0	0	0	76.4253	1.0141	1.0377	1.0080	0.8985
954.9926	0	0	0	0	83.8969	1.0100	1.1616	1.0415	0.9332
1096.4782	0	0	0	0	92.0988	1.0269	1.3877	1.0762	0.9439
1258.9254	0	0	0	0	101.1030	1.0577	1.6204	1.1083	0.9458
1445.4398	0	0	0	0	110.9870	1.0845	1.6728	1.1300	0.9535
1659.5869	0	0	0	0	121.8370	1.0905	1.3820	1.1372	0.9749
1905.4607	0	0	0	0	133.7480	1.0804	0.8081	1.1406	1.0130
					146.8240	1.0840	0.4575	1.1621	1.0715
					161.1770	1.1516	0.4883	1.2302	1.1695
					176.9350	1.3368	1.2749	1.3698	1.3448
					194.2320	1.6739	2.9267	1.5939	1.6413
					213.2210	2.1636	4.9101	1.9028	2.0895
					234.0660	2.7434	5.8917	2.2754	2.6675
					256.9480	3.2997	5.4599	2.6700	3.2859
					282.0680	3.6999	3.7915	3.0232	3.7997
					309.6440	3.8323	1.8329	3.2535	4.0560
					339.9160	3.6495	0.5237	3.2858	3.9600
					373.1470	3.1872	0.0730	3.0719	3.5174
					409.6260	2.5345	0.0026	2.6156	2.8185
					449.6720	1.8260	0	1.9881	2.0223
					493.6330	1.1811	0	1.3035	1.2850
					541.8920	0.6191	0	0.6644	0.6559
					594.8690	0.2407	0	0.2359	0.2466
					653.0250	0.0475	0	0.0425	0.0474

续表 3

粒级 2	含量(%)				粒级 1	含量(%)			
	24 cm	34 cm	43.5 cm	54.5 cm		24 cm	34 cm	43.5 cm	54.5 cm
					716.8660	0.0042	0	0.0031	0.0041
					786.9490	0	0	0	0
					863.8830	0	0	0	0
					948.3380	0	0	0	0
					1041.0500	0	0	0	0
					1142.8300	0	0	0	0
					1254.5500	0	0	0	0
					1377.2000	0	0	0	0
					1511.8400	0	0	0	0
					1659.6400	0	0	0	0
					1821.8900	0	0	0	0

注:粒级 2 指去除有机残体后沉积物样品粒级;粒级 1 指未去除有机残体时沉积物样品粒级。

为类似。可见,五大连池天池沉积物>83 μm 粒度组分与季风降水变化密切相关,可使用该组分粒度参数指示季风降水强弱变化。

3.2　季风降水变化

如上所述,天池沉积物>83 μm 有机残体组分对季风降水变化较为敏感,当季风降水强度增加时,有机残体含量增加且粒径增大。因此可将天池沉积物>83 μm 有机残体组分中值粒径作为夏季风降水指标,其值增大表明夏季风增强,降水增多,气候湿润;反之降水减少,气候干旱。

根据五大连池火山口湖沉积物>83 μm 组分的含量及中值粒径变化序列(图 6),我们重建了五大连池火山口湖早全新世夏季风降水演化历史。天池沉积物>83 μm 有机残体的粒径含量与中值粒径变化非常一致,两者呈显著正相关($R=0.93$,$P<0.0001$)。早全新世二者均呈现显著的千百年尺度振荡,其中可识别出~8.6 ka,~9.2 ka,~10.2 ka 和~11.6 ka 四次显著弱夏季风降水事件。考虑到年代不确定性,其中~11.6 ka 事件可能属于早全新世事件,而非新仙女木事件。

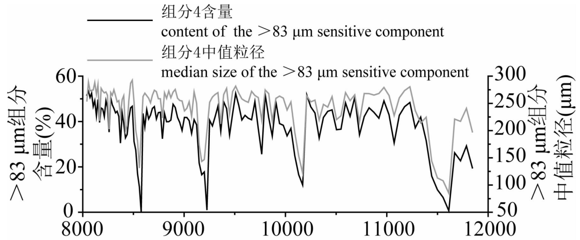

图 6　黑龙江五大连池火山口湖 TC1 沉积柱敏感粒级组分含量及中值粒径变化

Fig. 6　Variations in median size and content of sensitive component in Core TC1 from Wudalianchi Crater Lake in Heilongjiang Province

为深入探讨天池粒度记录的季风演化信息,将该记录与青海湖沉积(An Zhisheng et al., 2012)及哈尼泥炭记录(Hong Yetang et al., 2005)重建的夏季风指标进行对比(图 7)。天池粒度记录显示早全新世夏季风整体变化趋势不明显,与中国南方(Yang Yan et al., 2010; Dong Jinguo et al., 2010; Zhang Huiling et al., 2013; Huang Wei et al., 2016)和中国东北辽宁暖和洞(Wu Jiangying et al., 2011)等石笋记录的早全新世夏季风逐渐增强并不一致,可能由于不同指标的敏感性差异所致(Tan Ming et al., 2009),也可能是不同区域气候响应机制的差异所致。然而,天池沉积物粒度记录的早全新世千百年尺度弱夏季风事件在年代误差范围内与青海湖沉积夏季风指标低值及被用于重建夏季风降水的哈尼泥炭纤维素 $\delta^{13}C$ 低值均有较好对应关系,大量高分辨率洞穴石笋 $\delta^{18}O$ 序列中也记录了相应的弱夏季风事件,表明早全新世千百年尺度弱夏季风事件在我国季风区普遍存在。另外,值得注意的是,天池粒度记录的早全新世千百年尺度弱夏季风事件持续时间似乎明显短于其他气候记录事件的持续时间。

3.3　机制探讨

目前,多数研究者认为早全新世千百年尺度弱夏季风事件与北大西洋冰筏事件及太阳活动有关(Liu Xingxing et al., 2016)。天池沉积物粒度记录的早全新世四次千百年尺度弱夏季风事件与北大西洋四次冷事件(Bond et al., 2001)在年代误差范围内基本吻合,进一步表明早全新世千百年尺度弱夏季风事件与北大西洋冰筏事件密切相关。研究(Dykoski et al., 2005; An Zhisheng et al., 2012; Wang Shaowu et al., 2013)认为大量淡水爆发使北大西洋经向翻转流减弱,影响北大西洋气候及赤道

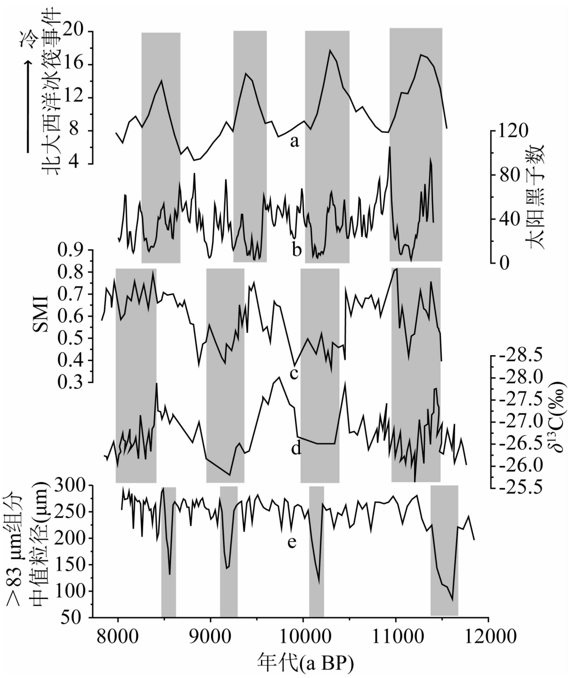

图 7 早全新世 TC1 孔敏感粒级组分中值粒径与其他气候记录对比

Fig. 7 Comparison of median size of the sensitive grain size component in Core TC1 and other climate records in early Holocene

(a)—北大西洋冰筏沉积记录(Bond et al., 2001);(b)—太阳黑子数(Solanki et al., 2004);(c)—夏季风指标(An Zhisheng et al., 2012);(d)—哈尼泥炭 δ^{13}C 记录(Hong Yetang et al., 2005);(e)—TC1 孔敏感粒级组分中值粒径

(a)—North Atlantic ice-raft record (Bond et al., 2001); (b)—Sunspot number (Solanki et al., 2004); (c)— Summer monsoon index (An Zhisheng et al., 2012); (d)—δ^{13}C record of Hani peat (Hong Yetang et al., 2005); (e)—Median size of sensitive component in Core TC1

辐合带(ITCZ)位置进而影响季风环流。天池沉积物粒度记录的弱夏季风事件在时间跨度上均明显短于我国季风区其他气候记录,可能是淡水爆发使ITCZ位置发生移动,通过影响热带季风进而影响较高纬度季风环流。季风信号从低纬传输至高纬,到达高纬时已相对较弱,致使事件持续时间较其他气候记录短。然而,这一现象出现的原因也有可能为沉积速率本身的变化以及指标的敏感程度不同,对上述解释仍需进一步验证。

中国大量夏季风指标序列的功率谱分析结果以及与^{14}C或^{10}Be记录对比分析结果均表明早全新世千百年尺度弱夏季风事件不论在周期上或变化趋势上都和太阳活动密切相关(Magny et al., 1995; Wang Yongjin et al., 2005; Yin Zhiqiang et al., 2014; Zhang Huasheng et al., 2016)。天池沉积物粒度记录的8.6 ka,9.2 ka,10.2 ka和11.6 ka弱季风事件恰好对应太阳黑子数低值(Solanki et al., 2004)(图6),即对应弱的太阳活动,进一步表明千百年尺度弱夏季风降水事件在一定程度上与太阳活动有关。

4 结论

结合五大连池火山口湖独特的地理位置及湖泊特征,根据其沉积物粒度数据分析及讨论结果,得到以下结论:

(1)沉积物中>83 μm敏感粒级组分为有机残体,其含量和粒度变化主要受季风降水影响。因此>83 μm粗粒级有机残体含量与中值粒径可作为东亚夏季风降水的有效代用指标,其值增大,指示夏季风增强,降雨增加,气候湿润;反之夏季风减弱,降雨减少。

(2)天池沉积物粒度序列记录了早全新世8.6 ka、9.2 ka、10.2 ka和11.6 ka四次千百年尺度的显著弱夏季风事件,这与中国洞穴石笋、东北哈尼泥炭及青海湖沉积物等记录的弱季风事件在年代误差范围内具有一致性,表明弱夏季风事件在我国季风区普遍存在。

(3)早全新世千百年尺度弱季风事件与北大西洋气候及太阳活动的变化密切相关。天池粒度记录的弱夏季风事件持续时间较其他记录短,可能是淡水爆发影响ITCZ位置,通过影响热带季风进而影响较高纬度季风环流,季风信号传输至高纬减弱,致使事件持续时间变短。但由于年代不确定性及分辨率不同,不同气候记录识别的弱夏季风事件往往不能精准对应,事件内部特征及变化趋势呈现一定差异,若要进行进一步深入探讨还需更多高分辨率、高定年精度气候记录进行对比。

致谢:感谢谢远云教授和另外一位匿名审稿专家提出的专业且有建设性意见和建议。

References

An Zhisheng, Colman S M, Zhou Weijian, Li Xiaoqiang, Brown E T, Timothy Jull A J, Cai Yanjun, Huang Yongsong, Lu Xuefeng, Chang Hong, Song Yougui, Sun Youbin, Xu Hai, Liu Weiguo, Jin Zhangdong, Liu Xiaodong, Cheng Peng, Liu Yu, Ai Li, Li Xiangzhong, Liu Xiuju, Yan Libin, Shi Zhengguo, Wang Xulong, Wu Feng, Qiang Xiaoke, Dong Jibao, Lu Fengyan, Xu Xinwen. 2012. Interplay between the Westerlies and Asian monsoon recorded in Lake Qinghai sediments since 32 ka. Scientific Reports, 2. doi: 10.1038/srep00619.

Blackford J J, Chambers F M. 1995. Proxy climate record for the last 1000 years from Irish blanket peat and a possible link to solar variability. Earth and Planetary Science Letters, 133(1): 145～150.

Bond G, Showers W, Cheseby M, Lotti R, Almasi P, deMenocal P, Priore P, Cullen H, Hajdas I, Bonani G. 1997. Apervasive millennial-scale cycle in North Atlantic Holocene and glacial climates. Science, 278(5341): 2402～2415.

Bond G, Kromer B, Beer J, Muscheler R, Evans M N, Showers W, Hoffmann S, Lotti-Bond R, Hajdas I, Bonani G. 2001. Persistent solar influence onNorth Atlantic climate during the Holocene. Science, 294(5549): 2130～2136.

Borgmark A. 2005. Holocene climate variability and periodicities in south-central Sweden, as interpreted from peat humification analysis. The Holocene, 15(3): 387～395.

Cai Binggui, Edwards R L, Cheng Hai, Tan Ming, Wang Xu, Liu Tungsheng. 2008. A dry episode during the Younger Dryas and centennial-scale weak monsoon events during the early Holocene: a high-resolution stalagmite record from southeast of the Loess Plateau, China. Geophysical Research Letters, 35(2): L02705.

Chen Fahu, Zhu Yan, Li Jijun, Shi Qi, Jin Liya, Wunemann B. 2001. Abrupt Holocene changes of the Asian monsoon at millennial-and centennial-scales: Evidence from lake sediment document in Minqin Basin, NW China. Chinese Science Bulletin, 46(23): 1942～1947.

Chen Qiao, Liu Dongyan, Chen Yingjun, Shen Xuhong, Jiang Jinjie, Li Xin, Jiang Xiaohua. 2013. Comparative analysis of grade-standard deviation method and factors analysis method for environmental sensitive factor analysis. Earth and Environment, 41(3): 319～325 (in Chinese with English abstract).

Dansgaard W, Johnsen S J, Clausen H B, Dahl-Jensen D, Gundestrup N S, Hammer C U, Hvidberg C S, Steffensen J P, Sveinbjörnsdottir, Jouzel J, Bond G. 1993. Evidence for general instability of past climate from a 250-kyr ice-core record. Nature, 364(6434): 218～220.

Dong Jinguo, Wang Yongjin, Cheng Hai, Hardt Ben, Edwards R L, Kong Xinggong, Wu Jiangying, Chen Shitao, Liu Dianbing, Jiang Xiuyang, Zhao Kan. 2010. A high-resolution stalagmite record of the Holocene East Asian monsoon from Mt Shennongjia, centralChina. The Holocene, 20(2): 257～264.

Duan Yi, Wu Yingzhong, Zhao Yang. 2016. Composition and hydrogen isotope of n-Alkanes in sediments fromGahai lake of Qinghai-Tibet Plateau, China and their implications for organic origin. Acta Geologica Sinica, 90(5): 1030～1039 (in Chinese with English abstract).

Dykoski C A, Edwards R L, Cheng Hai, Yuan Daoxian, Cai Yanjun, Zhang Meiliang, Lin Yushi, Qing Jiaming, An Zhisheng, Revenaugh J. 2005. A high-resolution, absolute-dated Holocene and deglacial Asian monsoon record fromDongge Cave, China. Earth and Planetary Science Letters, 233(1): 71～86.

Gui Zhifan, Xue Bin, Yao Shuchun, Wei Wenjia. 2011. Environmental changes of Wudalianchi lake inferred from lake sediments in the past century. Quaternary Sciences, 31(3): 544～553 (in Chinese with English abstract).

He Jishan, Liang Xing, Li Jing, Yang Jilong. 2015. Environmentally sensitive grain size extraction of deep hole sediment from Tianjin coastal plain and its significance. Earth Science (Journal of China University of Geosciences), 40(7): 1215～1225 (in Chinese with English abstract).

Hong Yetang, Hong Bing, Lin Qinghua, Shibata Y, Hirota M, Zhu Yongxuan, Leng Xuetian, Wang Yu, Wang Huijun, Yi Liang. 2005. Inverse phase oscillations between the East Asian andIndian Ocean summer monsoons during the last 12000 years and paleo-El Niño. Earth and Planetary Science Letters, 231(3): 337～346.

Hou Guangliang, Fang Xiuqi. 2011. Characteristics of Holocene temperature change inChina. Progress in Geography, 30(9): 1075～1080 (in Chinese with English abstract).

Huang Jie, Li Anchun, Wan Shiming. 2011. Sensitive grain-size records of Holocene East Asian summer monsoon in sediments of northern South China Sea slope. Quaternary Research, 75(3): 734～744.

Huang Wei, Wang Yongjin, Cheng Hai, Edwards R L, Shen Chuan-Chou, Liu Dianbing, Shao Qingfeng, Deng Chao, Zhang Zheqiu, Wang Quan. 2016. Multi-scale Holocene Asian monsoon variability deduced from a twin-stalagmite record in southwestern China. Quaternary Research, 86(1): 34～44.

Jouzel J, Genthon C, Lorius C, Petit J R, Barkov N L. 1987. Vostok ice core-A continuous isotope temperature record over the last climatic cycle (160,000 years). Nature, 329(6138): 403～408.

Li Chaozhou, Fu Jianli, Yi Liang, Zhou Xin, Wang Shubing, Jiang Fuchu. 2015. Millennial-scale Asian monsoon influenced Longjie Lake evolution during Marine Isotope Stage 3, upper stream of Changjiang (Yangtze) River, China. Advances in Meteorology, doi: 10.1155/2015/592894.

Li Huayong, Ming Qingzhong, Zhang Hucai, Duan Lizeng, Zhang Ziqiang. 2014. Paleoclimatic significance of grain-size from lacustrine sediments inChina. Scientific Journal of Earth Science, 4(2): 98～108 (in Chinese with English abstract).

Li Jiacai, Deng Youguo, Sun Juanjuan, Zheng Huasheng, Han Jian, Fan Ke, Li Chen, Wei Longming. 2015. Re-examining grain size variations in surface sediments from Guantouling Beach, Beihai. Geological Review, 61(suppl): 77～78 (in Chinese).

Li Suping, Li Jinfeng, Wu Zhenjie, Yao Jianxin. 2016. Climatic and environmental changes of Lugu lake area during the late Holocene. Acta Geologica Sinica, 90(8): 1998～2012 (in Chinese with English abstract).

Liu Jiali, Liu Qiang, Chu Guoqiang, Wu Jing, Liu Jiaqi. 2015. Sediment record at lake Sifangshan in the central-northern part of the Great Xing'an range, northeast China since 15.4 ka B. P. Quaternary Sciences, 35(4): 901～912 (in Chinese with English abstract).

Liu Jianbao, Chen Jianhui, Zhang Xiaojian, Li Yu, Rao Zhiguo, Chen Fahu. 2015. Holocene East Asian summer monsoon records in northern China and their inconsistency with Chinese stalagmite $\delta^{18}O$ records. Earth-Science Reviews, 148(1): 194～208.

Liu Qiang, Li Qian, Wang Luo, Chu Guoqiang. 2010. Stable carbon isotope record of bulk organic matter from a sediment core at moon lake in the middle part of the Daxing'an mountain range, northeast China during the last 21 ka. Quaternary Sciences, 30(6): 1069～1077 (in Chinese with English abstract).

Liu Siwen, Chu Guoqiang, Lai Zhongping. 2016. Determination of age and sediment rates using radionuclide ($^{210}Pb_{uns}$ and ^{137}Cs) dating in Inter-dune lake of the Badain Jaran desert, China. Acta Geologica Sinica, 90(8): 2013～2022 (in Chinese with English abstract).

Liu Xingxing, Vandenberghe J, An Zisheng, Li Ying, Jin Zhangdong, Dong Jibao, Sun Youbin. 2016. Grain size of Lake Qinghai sediments: Implications for riverine input and Holocene monsoon variability. Palaeogeography, Palaeoclimatology, Palaeoecology, 449(1): 41～51.

Liu Zhengyu, Wen Xinyu, Brady E C, Otto-Bliesner B, Yu Ge, Lu Huayu, Cheng Hai, Wang Yongjin, Zheng Weipeng, Ding Yihui, Edwards R L, Cheng Jun, Liu Wei, Yang Hao. 2014. Chinese cave records and the East Asia Summer Monsoon. Quaternary Science Reviews, 83(1): 115～128.

Liu Zhirong, Shen Jun, Huang Jingyi, Chen Yaofei. 2016. Grain size analysis of the late Pleistocene sediments inSanhe County, Hebei Province. Acta Geologica Sinica, 90(5): 997～1005 (in Chinese with English abstract).

Ma Chunmei, Zhu Cheng, Zheng Chaogui, Yin Qian, Zhao Zhiping. 2009. Climate changes in East China since the late-glacial inferred from high-resolution mountain peat humification records. Science in China Series D: Earth Sciences, 52(1): 118～131.

Magny M. 1995. Successive oceanic and solar forcing indicated by Younger Dryas and Early Holocene climatic oscillations in the Jura. Quaternary Research, 43(3): 279～285.

Mayewski P A, Rohling E E, Stager J C, Karlén W, Maasch K A, Meeker L D, Meyerson E A, Gasse F, van Kreveld S, Holmgren K, Lee-Thorp J, Rosqvist G, Rack F, Staubwasser M, Schneider R R, Steig E J. 2004. Holocene climate variability. Quaternary Research, 62(3): 243～255.

Peng Shuzhen, Hao Qingzhen, Wang Luo, Ding Min, Zhang Wei, Wang Yanan, Guo Zhengtang. 2016. Geochemical and grain-size evidence for the provenance of loess deposits in theCentral Shandong Mountains region, northern China. Quaternary Research, 85(2): 290～298.

Rasmussen S O, Vinther B M, Clausen H B, Andersen K K. 2007. Early Holocene climate oscillations recorded in three Greenland ice cores. Quaternary Science Reviews, 26(15): 1907～1914.

Reimer P J, Bard E, Bayliss A, Beck J W, Blackwell P G, Ramsey C B, Buck C E, Cheng Hai, Edwards R L, Friedrich M, Grootes P M, Guilderson T P, Haflidason H, Hajdas I, Hatté C, Heaton T J, Hoffmann D L, Hogg A G, Hughen K A, Kaiser K F, Kromer B, Manning S W, Niu Mu, Reimer R W, Richards D A, Scott E M, Southon J R, Staff R A, Turney C S M, van der Plicht J. 2013. IntCal13 and Marine13 radiocarbon age calibration curves 0～50,000 years cal BP. Radiocarbon, 55(4): 1869～1887.

Shen Baizhu, Lin Zhongda, Lu Riyu, Lian Yi. 2011. Circulation anomalies associated with interannual variation of early-and late-summer precipitation in Northeast China. Science China: Earth Sciences, 54(7): 1095～1104.

Solanki S K, Usoskin I G, Kromer B, Schüssler M, Beer J. 2004. Unusual activity of the Sun during recent decades compared to the previous 11,000 years. Nature, 431(7012): 1084～1087.

Tan Ming. 2009. Circulation effect: Climatic significance of the short term variability of the oxygen isotopes stalagmites from monsoonalChina—Dialogue between paleoclimate records and modern climate research. Quaternary Sciences, 29(5): 851～862 (in Chinese with English abstract).

Tan Ming. 2014. Circulation effect: response of precipitation $\delta^{18}O$ to the ENSO cycle in monsoon regions of China. Climate Dynamics, 42(3～4): 1067～1077.

Tu Luyao, Zhou Xin, Liu Yi, Cheng Wenhan, Sun Liguang. 2015. Re-analysis of sensitive grain size of coastal muddy sediments as proxy of winter monsoon strength: comparison with instrumental data. Quaternary Science, 35(6): 1393～1401 (in Chinese with English abstract).

Tu Luyao, Zhou Xin, Cheng Wenhan, Liu Xiaoyan, Yang Wenqing, Wang Yuhong. 2016. Holocene East Asian winter monsoon changes reconstructed by sensitive grain size of sediments from Chinese coastal seas: A review. Quaternary International, doi: 10.1016/j.quaint.2016.03.024.

Wang Ninglian, Yao Tandong, Thompson L G, Henderson K A, Davis M E. 2002. Evidence for cold events in the early Holocene from the Guliya ice core, Tibetan Plateau, China. Chinese Science Bulletin, 47(17): 1422～1427.

Wang Shaowu, Ge Quansheng, Wang Fang, Wen Xinyu, Huang Jianbin. 2013. Abruptclimate changes of Holocene. Chinese Geographical Science, 23(23): 1～12.

Wang Yongjin, Cheng Hai, Edwards R L, He Yaoqi, Kong Xinggong, An Zhisheng, WuJiangying, Kelly M J, Dykoski C A, Li Xiangdong. 2005. The Holocene Asian monsoon: links to solar changes and North Atlantic climate. Science, 308(5723): 854～857.

Wu Jiangying, Wang Yongjin, Dong Jinguo. 2011. Changes in East Asian summer monsoon during the Holocene recorded by stalagmite $\delta^{18}O$ records from Liaoning Province. Quaternary

Sciences, 31(6): 990～998 (in Chinese with English abstract).

Xiang Rong, Yang Zuosheng, Saito Y, Guo Zhigang, Fan Dejiang, Li Yunhai, Xiao Shangbin, Shi Xuefa, Chen Muhong. 2006. East Asia Winter Monsoon changes inferred from environmentally sensitive grain-size component records during the last 2300 years in mud area southwest off Cheju Island, ECS. Science in China Series D: Earth Sciences, 49(6): 604～614.

Xiao Shangbin, Li Anchun. 2005. A study on environmentally sensitive grain size population in inner shelf of theEast China sea. Acta Sedimentologica Sinica, 23(1): 122～129 (in Chinese with English abstract).

Xue Jibin, Zhong Wei. 2008. Variations in dust event reflected by grain-size component oflacustrine records in droughty area a case study on Barkol Lake, Xinjiang China. China. Acta Sedimentologica Sinica, 26(4): 647～654 (in Chinese with English abstract).

Yang Yan, Yuan Daoxian, Cheng Hai, Zhang Meiliang, Tan Jiaming, Lin Yushi, Zhu Xiaoyan, Edwards R L. 2010. Precise dating of abrupt shifts in the Asian monsoon during the last deglaciation based on stalagmite data from Yamen cave, Guizhou Province, China. Science China: Earth Sciences, 53(5): 633～641.

Yang Zuosheng, Chen Xiaohui. 2007. Centurial high resolution records of sediment grain-size variation in the mud area off the Changjiang (Yangtze River) restudy and its influential factors. Quaternary Sciences, 27(5): 690～699 (in Chinese with English abstract).

Yin Zhiqiang, Han Yanben, Wangbo. 2014. Possible response of climate to solar activity on millennial scale during the Holocene. Advances in Meteorogical Science and Technology, 4(4): 9～12 (in Chinese with English abstract).

Zhang Huasheng, Yin Jianjun, Cheng Hai, R Lawrence Edwards, Lin Shiyu, Tang Wei, Yang Hui, Tu Linling, Wang Hua, Pan Moucheng, Wu Xia. 2016. Discussion about the mechanism of the weak summer monsoon events during the early Holocene: a case study of precisely dated stalagmite record from Lianhua cave, Hunan province, China. Acta Sedimentologica Sinica, 34(2): 281～291 (in Chinese with English abstract).

Zhang Huiling, Yu Kefu, Zhao Jianxin, Feng Yuexing, Lin Yushi, Zhou Wei, Liu Guohui. 2013. East Asian Summer Monsoon variations in the past 12.5 ka: high-resolution δ^{18}O record from a precisely dated aragonite stalagmite in central China. Journal of Asian Earth Sciences, 73(1): 162～175.

Zhang Yinhuan, Yang Yan, Yang Xunlin, Yin Jianjun, Huang Fan, Ren Xiaofeng, Zhao Jingyao, Liu Xiao, Nie Xudong. 2015. Early Holocene monsoon evolution of high-resolution stalagmite δ^{18}O records: in Henan Laomu cave. Acta Sedimentologica Sinica, 33(1): 134～141 (in Chinese with English abstract).

Zheng Wenxin, Yang Guifang, Chen Zhenghong, Li Hui. 2015. Records of grain size characteristics and their environmental significances since the Late Glacial from Binggou loess section, Ningxia of monsoon margin. Geological Review, 61(suppl): 61～62 (in Chinese).

Zhou Xin, Yang Wenqing, Xiang Rong, Wang Yuhong, Sun Liguang. 2014. Re-examining the potential of using sensitive grain size of coastal muddy sediments as proxy of winter monsoon strength. Quaternary International, 333(1): 173～178.

Zhou Xin, Sun Liguang, Zhan Tao, Huang Wen, Zhou Xinying, Hao Qingzhen, Wang Yuhong, He Xiaoqing, Zhao Chao, Z hang Jun, Qiao Yansong, Ge Junyi, Yan Pei, Yan Qing, Shao Da, Chu Zhuding, Yang Wenqing, Smol John. 2016. Time-transgressive Onset of the Holocene Optimum in the East Asian Monsoon Region. Earth and Planetary Science Letters, 456(1): 39～46.

参　考　文　献

陈桥，刘东艳，陈颖军，申旭红，蒋金杰，李欣，姜晓华. 2013. 粒级—标准偏差法和主成分因子分析法在粒度敏感因子提取中的对比. 地球与环境，41(3)：319～325.

段毅，吴应忠，赵阳. 2016. 青藏高原东北部尕海湖沉积物中正构烷烃及其氢同位素组成与有机质源指示意义. 地质学报，90(5)：1030～1039.

桂智凡，薛滨，姚书春，魏文佳. 2011. 黑龙江省五大连池近百年环境变化研究. 第四纪研究，31(3)：544～553.

何继山，梁杏，李静，杨吉龙. 2015. 天津滨海平原区深孔沉积物环境敏感粒度提取及其意义. 地球科学(中国地质大学学报)，40(7)：1215～1225.

侯光良，方修琦. 2011. 中国全新世气温变化特征. 地理科学进展，30(9)：1075～1080.

李华勇，明庆忠，张虎才，段立曾，张自强. 2014. 中国湖泊沉积物中的粒度变化及其古气候和古环境指示意义. 地球科学期刊：中英文版，4(2)：98～108.

黎家财，邓友国，孙娟娟，郑华盛，韩见，范可，李晨，韦龙明. 2015. 北海冠头岭沙滩表层沉积物粒度变化再研究. 地质论评，61(增刊)：77～78.

李素萍，李金锋，武振杰，姚建新. 2016. 泸沽湖地区晚全新世气候和环境演变. 地质学报，90(8)：1998～2012.

刘嘉丽，刘强，储国强，伍婧，刘嘉麒. 2015. 大兴安岭四方山天池15.4 ka B. P. 以来湖泊沉积记录. 第四纪研究，35(4)：901～912.

刘强，李倩，旺罗，储国强. 2010. 21 ka B. P. 以来大兴安岭中段月亮湖沉积物全岩有机碳同位素组成变化及其古气候意义. 第四纪研究，30(6)：1069～1077.

刘斯文，储国强，赖忠平. 2016. 放射性核素$^{210}Pb_{uns}$、^{137}Cs测定巴丹吉林沙漠湖泊岩心的年代及沉积速率. 地质学报，90(8)：2013～2022.

刘智荣，沈军，黄静宜，陈耀飞. 2016. 河北三河晚更新世地层粒度特征分析. 地质学报，90(5)：997～1005.

谭明. 2009. 环流效应：中国季风区石笋氧同位素短尺度变化的气候意义——古气候记录与现代气候研究的一次对话. 第四纪研究，29(5)：851～862.

涂路遥，周鑫，刘毅，程文瀚，孙立广. 2015. 近海泥质沉积物敏感粒径作为冬季风强度指标的再研究：与器测数据的对比. 第四

纪研究，35(6)：1393～1401.
吴江滢，汪永进，董进国. 2011. 全新世东亚夏季风演化的辽宁暖和洞石笋 $\delta^{18}O$ 记录. 第四纪研究，31(6)：990～998.
肖尚斌，李安春. 2005. 东海内陆家泥区沉积物的环境敏感粒度组分. 沉积学报，23(1)：122～129.
薛积彬，钟巍. 2008. 干旱区湖泊沉积物粒度组分记录的区域沙尘活动历史：以新疆巴里坤湖为例. 沉积学报，26(4)：647～654.
杨作升，陈晓辉. 2007. 百年来长江口泥质区高分辨率沉积粒度变化及影响因素探讨. 第四纪研究，27(5)：690～699.
尹志强，韩延本，王博. 2014. 全新世气候对千年尺度太阳活动的可能响应. 气象科技进展，4(4)：9～12.
张华生，殷建军，程海，Edwards R L，林玉石，唐伟，杨会，涂林玲，王华，潘谋成，吴夏. 2016. 全新世早期弱夏季风事件的精确定位及机制探讨——以湖南莲花洞 LHD5 石笋为例. 沉积学报，34(2)：281～291.
张银环，杨琰，杨勋林，殷建军，黄帆，任小凤，赵景耀，刘肖，聂旭东. 2015. 早全新季风演化的高分辨率石笋 $\delta^{18}O$ 记录研究——以河南老母洞石笋为例. 沉积学报，33(1)：134～141.
郑文欣，杨桂芳，陈正洪，李慧. 2015. 季风边缘区宁夏兵沟剖面晚冰期以来黄土粒度特征及其环境意义. 地质论评，61(增刊)：61～62.

Grain-size of Organic Debris in Sediments from Wudalianchi Crater Lake in Heilongjiang Province Record the Evolution of Summer Monsoon Precipitation at Millennial- to Centennial-Scale in the Early Holocene

LIU Xiaoyan[1)], ZHAN Tao[2)], LIU Lian[3)], ZHOU Xin[1)], QIAO Yansong[4)], TU Luyao[1)], MA Yongfa[2)], JIANG Xia[5)], ZHANG Jun[2)], LOU Benjun[2)]

1) *School of Earth and Space Sciences, University of Science and Technology of China, Hefei*, 230026;
2) *The Second Hydrogeology and Engineering Geology Prospecting Institute of Heilongjiang Province, Haerbin*, 150030;
3) *Chinese Academy of Geological Sciences, Beijing*, 100037;
4) *Institute of Geomechanics, Chinese Academy of Geological Sciences, Beijing*, 100081;
5) *Heilongjiang Bureau of Geology & Mineral Resources, Haerbin*, 150036

Abstract

Millennial- to centennial-scale climate events in the early Holocene have been detected from numerous geological records in China, but records in high latitudes are still limited. Therefore, it could contribute to this research if such records are reconstructed in higher latitude regions of China. In the present study, grain sizes of a sediment core retrieved from a crater lake in Northeast China were analyzed. Sensitive grain size component of >83 μm was extracted by analyzing the grain size versus standard deviation curve of sediment, organic debris was not excluded. This component was mainly organic debris and can be used as a proxy of summer monsoon precipitation. Based on chronology from precise ^{14}C dates and the results of grain size analysis, a sequence of early Holocene summer monsoon precipitation in Northeast China was reconstructed. The results indicate that early Holocene monsoon precipitation in Northeast China fluctuated frequently with four millennial to centennial weak events of summer monsoon at ～8.6, 9.2, 10.2 and 11.6 ka BP. All of these weak monsoon intervals corresponded well with those in other climate records within chronological errors, e.g. records from the monsoon regions of China, North Atlantic ice-raft events and the solar activity records. The synchronicity of these records suggests widely spread drought events at millennial- to centennial-scale in the monsoon regions of China, and might link closely to the North Atlantic ice-raft events and solar activity. However, the durations of the four weak summer monsoon precipitation events recorded by grain sizes in the Wudalianchi lake sediments were significantly shorter than those in other climate records. One possible explanation is that the North Atlantic ice-raft events impacted high latitude regions via summer monsoon, while monsoon signal weakened gradually from low latitudes to high latitudes, resulting in the shorter duration of the events in our record.

Key words: Early Holocene; crater lake; sensitive grain size; weak summer monsoon events; Northeast China